RESEARCH PAPER

Electrical Conductivity of the Molten and Glassy States of the Li$_2$(O, Cl$_2$, I$_2$)-B$_2$O$_3$ System

Omid Banapour Ghaffari, Bijan Eftekhari Yekta*

* Beftekhari@iust.ac.ir

School of Metallurgy and Materials Engineering, Iran University of Science and Technology, Narmak, Tehran 1684613114, Iran

Abstract: *Glasses within the B$_2$O$_3$-Li$_2$(O, Cl$_2$, I$_2$) system were fabricated using the conventional melt-quenching technique. Subsequently, an assessment was conducted to determine the conductivity of the molten and glassy states of these compositions. X-ray diffractometry (XRD) and simultaneous thermal analysis (STA) were employed to investigate the thermal and crystallization properties of the glasses. The measurement of electrical conductivity in the molten state was conducted within a temperature range of 863 to 973 K. Subsequently, the activation energy associated with the conductivity of the samples was calculated based on the data acquired from ionic conduction. The computed activation energy was found to be around 32 kcal/mol. Electrical conductivity measurements were also conducted in glassy states. The electrochemical impedance spectroscopy (EIS) method was employed to determine this particular characteristic. The influence of temperature on ionic conductivity was significant in the molten state, but at lower temperatures, additional factors like mixing different anions, known as the "mixed anions effect," became important. The experimental findings indicate that the introduction of LiI and LiCl into the B$_2$O$_3$-Li$_2$O base glass system (with a composition of 75 mol% B$_2$O$_3$, 10 mol% Li$_2$O, 7.5 mol% LiI, and 7.5 mol% LiCl) leads to a significant enhancement in the ionic conductivity of the glass. Specifically, the measured ionic conductivity at 300 K increases from 3.2×10^{-8} S.cm^{-1} to 1.4×10^{-7} S.cm^{-1}.*

Keywords: *Ion conduction in glass melts, Ionic conduction activation energy, Mixed anion effect, Electrochemical impedance spectroscopy, All-solid-state electrolyte.*

1. INTRODUCTION

The growing demand for energy storage systems that are both renewable and cost-effective has prompted extensive research efforts aimed at enhancing battery technology. Batteries serve as the primary energy source for a wide range of electronic devices, including cell phones, laptops, and medical equipment. The search for of battery materials with high energy density, extended cycling life, and enhanced safety is of great importance. Currently, the lithium-ion battery stands as the most energy-dense battery, although the conventional lead-acid battery remains cost-effective. Despite the economic viability of lithium batteries, they provide a prospective fire risk as a result of metallic lithium dendrite shorts occurring within the liquid electrolyte, spanning from the anode to the cathode [1-5]. Solid electrolytes have the potential to provide a resolution to this problem. Moreover, the utilization of a solid-state electrolyte has the potential to significantly enhance the energy density. Nevertheless, an important obstacle lies in identifying solid electrolytes that possess sufficient alkali-ion conductivities. Fast ion-conducting glasses have the potential to serve as a solid-state electrolyte in advanced battery technologies of the future [6-11]. Binary lithium borate glasses and other fast-ion conductive oxide glasses with conductivities of ~10^{-8} or 10^{-9} S/cm are not adequately conductive for commercial use [12-16]. The rise in ionic conductivity can be attributed to several factors. Firstly, a higher concentration of alkali ions has been observed to enhance the conductivity. Secondly, the process of quick quenching has been found to have a positive effect on conductivity. Additionally, the use of mixed glass formers and the addition of alkali halide salts (known as the mixed anion effect) have also been shown to contribute to an increase in ionic conductivity [17-24]. In this study, the latter factor has been investigated. Also, more information about ion conduction behavior can be obtained from the molten state. Studying the ion conductivity in the molten state will give insight into the relationships between the molten and glassy structures. It has been observed that a molten sample shows a higher conductivity and lower activation energy for conductivity compared to its solid-state counterpart [25, 26]. It means that during the solidification process, a

drastic drop in conductivity occurs. Since glass generally obtains its structure from the rapid cooling of its melt, its structure is highly similar to its melt; thus, conductivity is a structure-related property, and the conductivity of the glass entirely depends on the conductivity of the melt [27-29]. On the other hand, ion conduction in the molten state has specific applications like high-temperature liquid electrolytes and high-temperature batteries for geothermal and oil and gas borehole applications [30-32].

This paper provides a framework for comprehending the effects of mixed anion effects and temperature on the electrical conductivity of the molten and glassy $Li_2(O, Cl_2, I_2)$-B_2O_3 system. In summary, the following are the significant contributions of this study: (i) The ion conduction in the molten state of the $Li_2(O, Cl_2, I_2)$-B_2O_3 system was measured with a customized set-up, and (ii) The activation energy of ionic conduction associated with every specimen was calculated. (iii) The distinction between ionic conductivity at elevated temperatures (molten state) and ambient temperatures (glassy state) was examined.

2. EXPERIMENTAL PROCEDURES

2.1. Materials and Methods

Table 1 displays the glass compositions formulated for this study. The mole ratio of lithium-ion, the primary charge carrier, remained constant across all samples, whereas the amounts of anions, i.e., O^{2-}, Cl^-, and I^-, varied among the samples.

The thermal behavior of the glass batches was studied using an STA (BaHR503) so that the probable evaporation of the glass batches could be studied. To synthesize the glasses, Sigma-Aldrich sources like lithium carbonate (554-13-2, purity ≥98%), lithium chloride (7447-41-8, purity ≥99%), lithium iodide (10377-51-2, purity ≥99%), and boric acid (10043-35-3, purity ≥99%) were used.

Using coaxial cylindrical electrodes, the electrical conductivity of the base composition, which

included 17.5 Li_2O and 82.5 B_2O_3 (mol%), was assessed in the molten state between 973 K and a temperature just below its glass transition temperature (833 K). The method described by Schiefelbein et al. [33, 34] was used to measure the specific resistivity. At 1023 K, the glass batches were melted. Using a stepper motor, coaxial cylindrical electrodes were then inserted into the melt at a predetermined depth. During the experiment, an alternating voltage was given to the electrodes while maintaining a constant temperature, and the current flowing through the melt was measured. The heating current was temporarily cut off throughout each test to eliminate induction noise from the furnace. For the lower temperatures and other batches, the same procedure was performed. It is important to note that to prevent the vitalization of raw materials, it is advisable to conduct measurements promptly. Figure 1 illustrates the setup used to measure the conductivity of the melts.

Then, the melt was cast into a cylindrical mold with a diameter of 20 mm and depth of 2 mm and quenched to room temperature. The glass samples were transparent and showed no visual signs of crystallization. The phase analysis of the samples was determined by X-ray powder diffraction (XRD, Bourevestnik, DRON-8), using CuKα radiation. The patterns were scanned in the 2θ range of 10-80°.

2.2. Ionic Conductivity of the Glasses

The glass spices with a diameter of 20 mm and thickness of 2 mm were polished to optical transparency and sputtered with gold electrodes with a diameter of 20 mm and they were loaded into a puck-like, sealed sample holder. The complex impedance spectrum was measured using a Princeton Parstat2273 impedance spectrometer from 1 mHz to 1 MHz. To prevent polarization, the DC conductivity was determined from AC measurements over a range of frequencies. The DC conductivities in this research were determined by fitting the complex impedance arc using Equation 1.

Table 1. Chemical composition of the prepared glasses (mol.%)

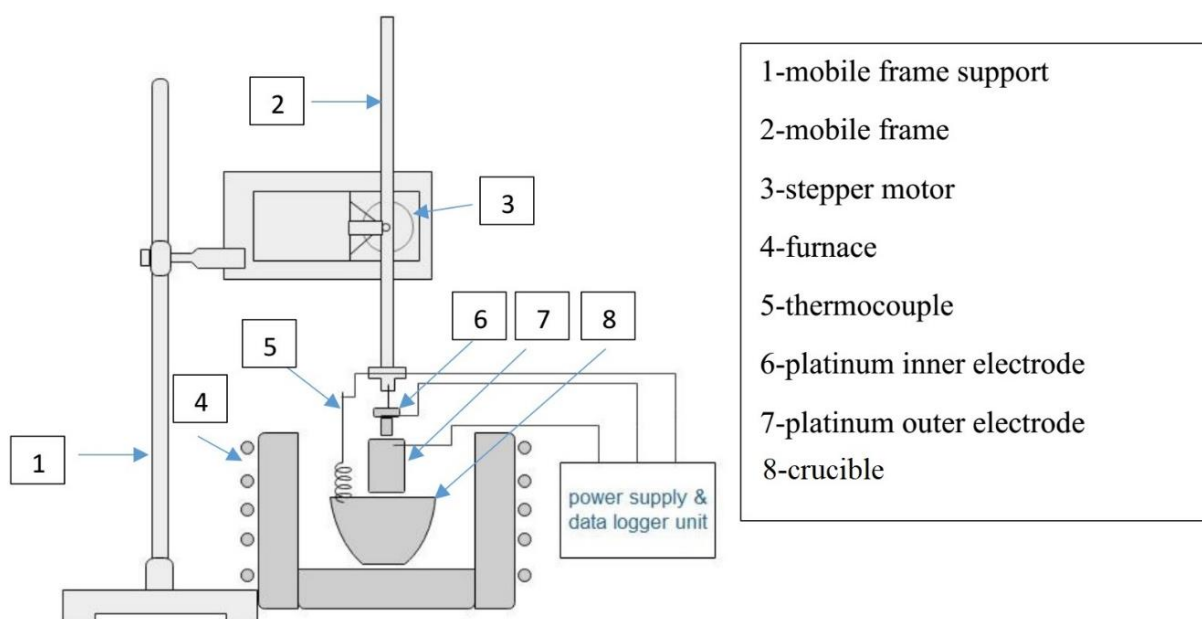| Sample code	Li$_2$O	LiCl	LiI	B$_2$O$_3$
B$_{75}$ O$_{10}$Cl$_{15}$	10	15	-	75
B$_{75}$ O$_{10}$I$_{15}$	10	-	15	75
B$_{75}$O$_{10}$Cl$_{7.5}$I$_{7.5}$	10	7.5	7.5	75
B$_{82.5}$ O$_{17.5}$	17.5	-	-	82.5

2

Fig. 1. Schematic of the setup assembly used to measure the conductivity of the samples in the molten state.

In this equation, a resistor in parallel with a constant phase element, Q, is used as the equivalent circuit to model the impedance, Z, where i is $\sqrt{}$-1, ω is the angular frequency, and n is an exponent that ranges from 0 to 1. Once the bulk resistance is determined, the DC conductivity, σ_{DC}, can be determined with the sample thickness, τ, and electrode area, A, using Equation 2.

$$Z = \frac{R}{1+RQ(i\omega)^n} \qquad (1)$$

$$\sigma_{DC} = \frac{1}{R} \times \frac{\tau}{A} \qquad (2)$$

3. RESULTS AND DISCUSSION

3.1. Thermal Analysis of the Glass Batches

Before preparing the melt and measuring its conductivity, it is necessary to know the weight loss associated with the evaporation of the elements present in the glass batches. This weight loss can be determined by conducting a thermogravimetric analysis (TGA) on the glass batches. It is also required to identify the melting range and possibility of thermal phase transition in the batch. Therefore, the thermal behavior of the batches was studied by the STA (Figure 2). It was observed that there was approximately 4 wt.% loss after melting the samples (~450°C) up to 800°C, this weight loss may be due to the evaporation of some constituents of the batches and can change the glass composition. Two endothermic peaks are observed in the STA

thermographs of the base glass batch, i.e., $B_{82.5}O_{17.5}$.
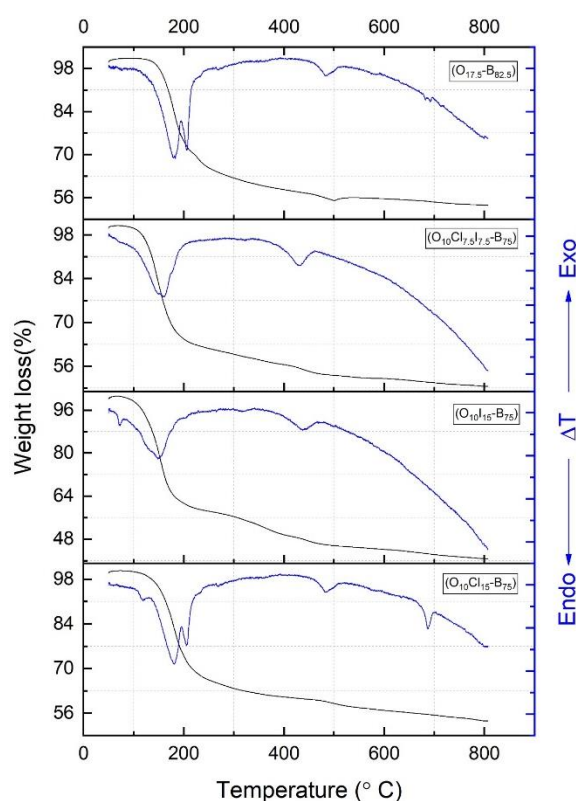

Fig. 2. STA thermographs of the prepared glass batches

The sharp peak with a considerable weight loss at the temperature range of 170°C to 220°C was attributed to the melting and dehydration of acid

boric, which is associated with the evaporation of its O-H groups [35]. The other result of this reaction is the formation of boron oxide, which melts at approximately 450°C. Thus, the second peak at approximately 435°C was attributed to the melting of B_2O_3, which depending on the batch composition has occurred in the temperature range of 420°C to 445°C in other thermographs. There is another endothermic peak in the batch sample $B_{82.5} O_{17.5}$, which contained the highest amount of lithium carbonate, at approximately 680°C. It was attributed to the melting and/or dissolving of lithium carbonate in the borate glass phase.

3.2. Phase Analysis

The absence of distinct diffraction peaks observed in the X-ray diffraction (XRD) patterns suggests that the examined glasses exhibit an amorphous phase at the point of XRD view, as depicted in Figure 3.
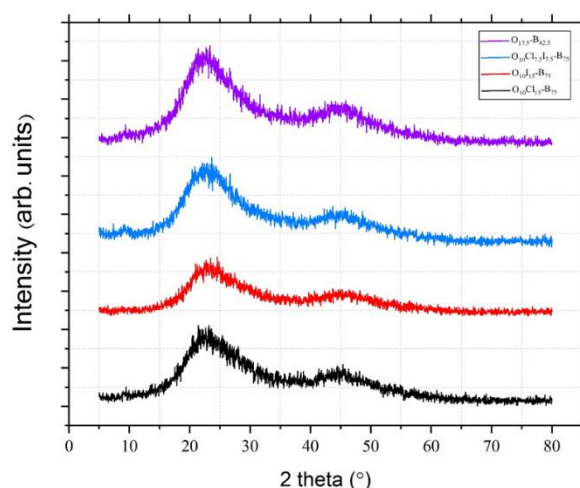

Fig. 3. XRD pattern of the prepared glass sample

This lack of sharp peaks implies the absence of a well-defined long-range atomic arrangement. Based on the data presented in Figure 3, it can be noted that the X-ray diffraction (XRD) patterns of the four glass samples have a notable similarity. Additionally, two distinct broad humps are prominently evident. The initial prominent peak was observed within the region of $15° < 2\theta < 30°$, providing robust evidence for the amorphous characteristics (namely, short-range order) shown by all the glass specimens. The determination of medium-range order can be achieved by analyzing X-ray diffraction (XRD) patterns, which may display either a pre-hump on the low-angle side of the primary peak or a more pronounced first diffraction peak [36]. Hence, an additional wide band exhibiting reduced intensity was detected within the angular span of 40–50°, indicating the existence of another phase characterized by medium-range structural organization. The presence of two distinct broad bands in sodium borate glasses has also been observed [37, 38].

3.3. Electrical Conductivity Measurement

3.3.1. Molten-state electrical conductivity

As shown in Figure 4, Figure 5, Figure 6, and Figure 7, with increasing the temperature from 823 to 973 K, the electrical conductivity of the samples increases exponentially, as was expected. This suggests that the molten-state conductivity of the composition is thermally activated, and may be attributed to the mobility of charge carriers within the material. It is known that the electrical conductivity of a glass melt obeys the following Arrhenius' law:

$$\sigma = \sigma_{\circ} \exp\left(-\frac{\Delta E}{RT}\right) \qquad (3)$$

Where $\sigma_{\circ}$ is a constant corresponding to the expected value of electrical conductivity at temperature tending to infinity, *T is* the absolute temperature, *R* gas constant, and ΔE *is* the activation energy of ionic conduction describing the height of potential barriers between two adjacent possible positions of current carriers in a liquid or glass.
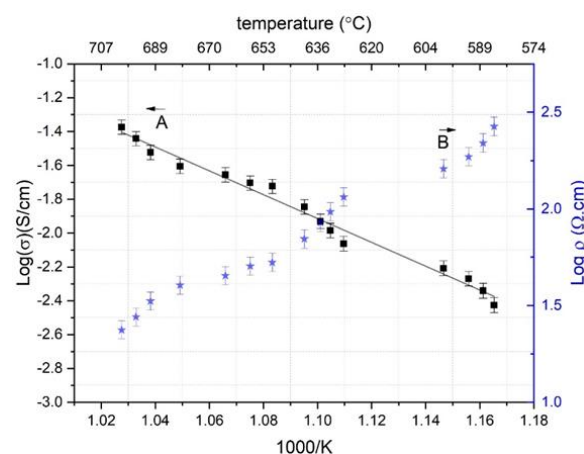

Fig. 4. The measured ionic conductivity of the molten glass $B_{82.5} O_{17.5}$, which nominally contained $17.5Li_2O +82B_2O_3$ (mol%) with temperature. curve (A) shows the conductivity as a function of temperature, where the experimental errors are evolving. The data in the curve (B) are the logarithmic specific resistivity with temperature

As mentioned for all samples, the conductivity increases in a linear fashion over a log(σ) vs. 1/T plot, following an Arrhenius-type behavior, so the activation energy, ΔE, of glass melts is calculated using equation 3 and illustrated in Error! Reference source not found..

their sites. So, the reduction in electrostatic bonding energy ultimately increases electrical conductivity. Also, by increasing the temperature, the viscosity of the glass melts is reduced exponentially, and as a result, the strain energy needed for the motion of ions is reduced and helps to improve electrical conductivity.
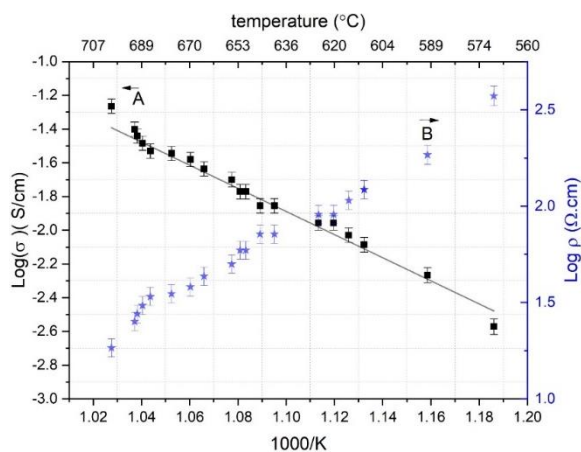

Fig. 5. The measured ionic conductivity for the molten glass composition is 10% Li_2O + 15% $LiCl$ + 75% B_2O_3. Curve (A) shows the conductivity plotted concerning temperature, where the experimental errors are evolving. The data in the curve (B) are the logarithmic special resistivity concerning temperature
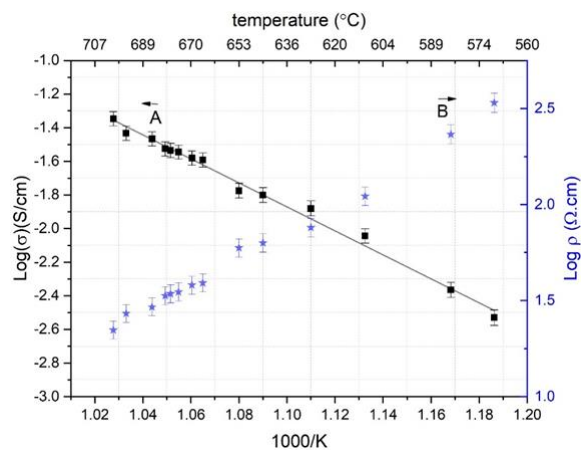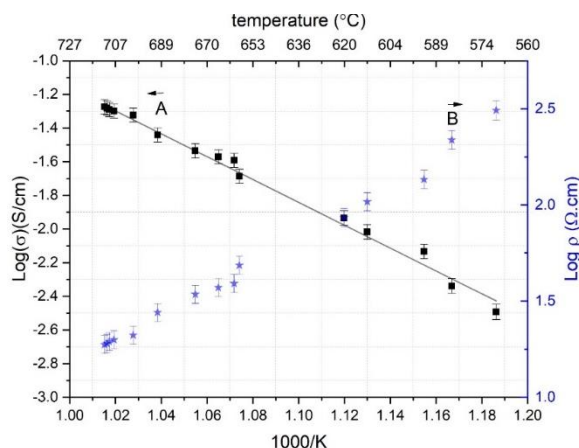

Fig. 7. The measured ionic conductivity for the molten glass composition is 10% Li_2O 7.5% $LiCl$ + 7.5% LiI + 75% B_2O_3. Curve (A) shows the conductivity plotted concerning temperature, where the experimental errors are evolving. The data in the curve (B) are the logarithmic special resistivity concerning temperature

Fig. 6. The measured ionic conductivity for the molten glass composition is 10% Li_2O + 15% LiI + 75% B_2O_3. Curve (A) shows the conductivity plotted concerning temperature, where the experimental errors are evolving. The data in the curve (B) are the logarithmic special resistivity concerning temperature
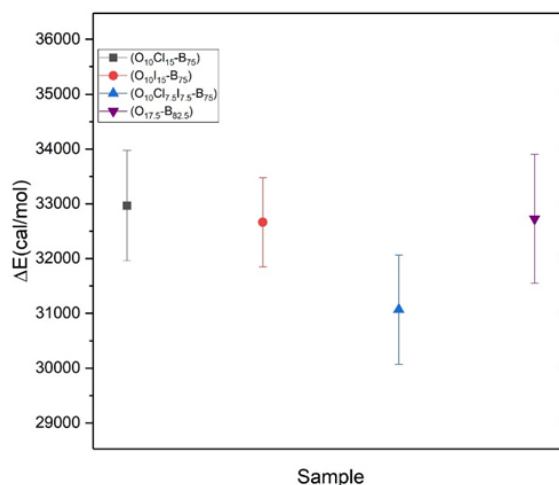

Fig. 8. The calculated activation energy, ΔE, of the molten glass batches.

3.3.2. Glassy-state electrical conductivity measurement

The complex impedance fitting arcs of the samples are shown in Error! Reference source not found.. The direct current (DC) conductivity of each glass sample at 300 K was found by fitting

Temperature increases the mobility of ions through more dilation in the glass structure and the expansion of conduction channels in the structure. On the other hand, the temperature increases the length of bonding links and reduces the bonding energy between the floating ions and

the complex impedance arc using Equation 1. The resistance of the sample is found through an AC experiment using the Nyquist plot, where the real and imaginary parts of the impedance were plotted on the x and y axes, respectively. For a parallel R-C circuit, semicircular arcs are expected. In equation 1, the constant phase element (CPE) explains these semicircular arcs' recession. Frequency dispersion in the glass samples is the direct explanation of this recession [39, 40]. The arcs in the Nyquist plot (see Error! Reference source not found.) are due to the bulk response of the resistive (R) and capacitive (C) behavior of the glass samples, and the polarization "tail" at low frequency arises from the space charge polarization, where the Li^+ ions can accumulate on the blocking electrodes and balance the bias voltage. Once the bulk resistance is determined, the DC conductivity, σ_{DC}, can be calculated using equation 2 which represents the DC conductivity (σ_{DC}) of each sample. According to the Anderson-Stuart Model [20] in the glassy state, conductivity is controlled by the activation energy. This physical quantity is interpreted as the energy barrier that must be overcome for an ionic charge carrier to jump to an adjoining site. The activation energy is a summation of the energy barrier related to squeezing pathways (ΔE_b) and energy to move through a doorway between adjacent charge-compensating sites (ΔE_s), the combination of these two energy barriers yields activation energy of ionic co described ($\Delta E_a = \Delta E_b + \Delta E_s$).

This model further suggested that by using equation 4, the binding energy can be approximated, where β is the finite displacement factor, ΔE_c is the columbic energy, γ is the covalency parameter and is equal to the dielectric constant, r_0 is the radius of the anion (Cl^-, I^- and O^{2-}), r is the radius of the cation (Li^+), z_0 and z are the valence of the anion and cation respectively. Likewise, using equation 5, the strain energy was approximated, where r_D is the doorway radius, r is the radius of the cation, and G is the shear modulus. Although many authors have proposed modifications and variations to improve the Anderson-Stuart model [16, 21], the concept of activation energy consisting of binding and strain energies has remained constant.

$$\Delta E_b = \Delta E_c \sim \frac{\beta z z_0 e^2}{\gamma(r+r_0)} \qquad (4)$$

$$\Delta E_s = 4\pi G r_D (r - r_D)^2 \qquad (5)$$

The Anderson-Stuart model suggests that substituting the larger anion for a smaller one will increase the doorway radius. Additionally, as the anion's radius grows, its effective nuclear charge drops, lowering the energy barrier associated with passing through a doorway (ΔE_s). These two parameters improve ion conduction, therefore replacing LiCl or LiI with Li_2O in the base glass system (17.5% Li_2O- 82.5% B_2O_3), where they have larger anion radii than O^{2-} in Li_2O, increased electrical conductivity (in sample $O_{10}Cl_{15}$-B_{75} or $O_{10}I_{15}$-B_{75}, respectively). note that the mole ratio of the charge carrier (Li^+) remained constant for all samples, on the other hand, the addition of LiCl and LiI simultaneously not only resulted in the replacement of bigger radius anions with smaller ones but also existing different kinds of anions helped site polarization which increased the ion conduction in sample $O_{10}Cl_{7.5}I_{7.5}$-B_{75}.
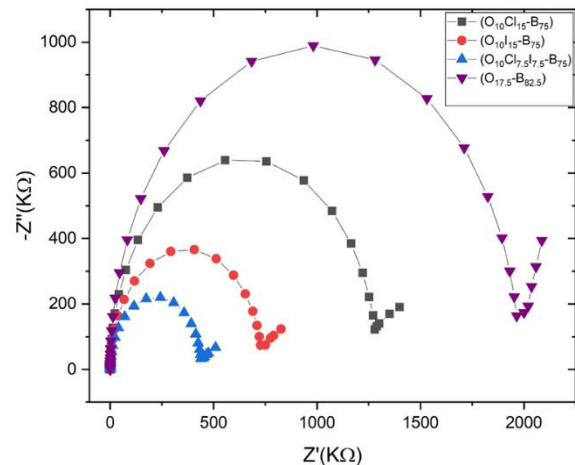
Fig. 9. Nyquist plot of the complex impedance for different glass samples at 300 K.

Table 2. The conductivity of the glass samples at 300 K calculated from EIS

Sample	conductivity at 300 K(S.cm^{-1})
$O_{10}Cl_{15}$-B_{75}	4.933×10^{-8}
$O_{10}I_{15}$-B_{75}	8.670×10^{-8}
$O_{10}Cl_{7.5}I_{7.5}$-B_{75}	1.443×10^{-7}
$O_{17.5}$-$B_{82.5}$	3.220×10^{-8}

4. CONCLUSIONS

The conductivity in the molten state, due to its structural relationship and its high similarity to the structure of the glass, is important, and temperature is a key factor in the electrical conductivity in the glass and its melt, and with increasing temperature, conductivity increases

6

exponentially. The present investigation involved the measurement of ionic conductivity in the $Li_2(O, Cl_2, I_2)$-B_2O_3 system throughout a broad temperature range (ranging from 863 K to 973 K) with a specifically designed experimental setup. Following this, the conduction activation energy was calculated to be approximately 32 kcal/mol based on the data collected from the ionic conductivity of the melts. The research revealed a notable disparity in ionic conductivity between the molten and glassy states at room temperature, with the former exhibiting considerably greater levels. This implies that the temperature-dependent mobility of charged particles, specifically ions, results in enhanced ionic conductivity when the substance is in a molten state. Moreover, this discovery holds significant ramifications for applications that necessitate conductivity at elevated temperatures, such as in the field of solid-state batteries or molten salt reactors. It has been observed that the conductivity and activation energy of different anions in molten samples are approximately consistent at high temperatures. This factor has a limited influence on the control of ion conduction. However, at lower temperatures, this factor can significantly enhance performance. Furthermore, in the glassy state, the incorporation of LiI salt exhibits a higher enhancement in conductivity compared to LiCl. Moreover, the simultaneous addition of both LiCl and LiI salts demonstrates the highest level of conduction. More specifically, the inclusion of LiI, LiCl, and the combination of LiCl and LiI together increased the ionic conductivity of the glassy state. The conductivity values were measured to be 3.220×10^{-8}, 8.670×10^{-8}, 3.220×10^{-8}, and 1.443×10^{-7}, respectively.

REFERENCES

[1]. Crabtree, G.W. and N.S. Lewis, Solar energy conversion. Physics Today, 2007. 60(3): p. 37-42.

[2]. Dollé, M., L. Sannier, B. Beaudoin, M. Trentin, and J.-M. Tarascon, Live scanning electron microscope observations of dendritic growth in lithium/polymer cells. Electrochemical and Solid State Letters, 2002. 5(12): p. A286.

[3]. Ohara, K., A. Mitsui, M. Mori, Y. Onodera, S. Shiotani, Y. Koyama, Y. Orikasa, M. Murakami, K. Shimoda, and K. Mori, Structural and electronic features of binary Li2S-P2S5 glasses. Scientific Reports, 2016. 6(1): p. 1-9.

[4]. Lin, Z. and C. Liang, Lithium–sulfur batteries: from liquid to solid cells. Journal of Materials Chemistry A, 2015. 3(3): p. 936-958.

[5]. Zhang, L., Y. Liu, Y. You, A. Vinu, and L. Mai, NASICONs-type solid-state electrolytes: The history, physicochemical properties, and challenges. Interdisciplinary Materials, 2023. 2(1): p. 91-110.

[6]. Choi, S., M. Eom, C. Park, S. Son, G. Lee, and D. Shin, Effect of Li2SO4 on the properties of Li2S–P2S5 glass-ceramic solid electrolytes. Ceramics International, 2016. 42(6): p. 6738-6742.

[7]. Li, J. and R. Wang, Recent advances in the interfacial stability, design and in situ characterization of garnet-type $Li_7La_3Zr_2O_{12}$ solid-state electrolytes based lithium metal batteries. Ceramics International, 2021. 47(10): p. 13280-13290.

[8]. Berbano, S.S., M. Mirsaneh, M.T. Lanagan, and C.A. Randall, Lithium Thiophosphate Glasses and Glass–Ceramics as Solid Electrolytes: Processing, Microstructure, and Properties. International Journal of Applied Glass Science, 2013. 4(4): p. 414-425.

[9]. Dewald, G.F., S. Ohno, M.A. Kraft, R. Koerver, P. Till, N.M. Vargas-Barbosa, J.R. Janek, and W.G. Zeier, Experimental assessment of the practical oxidative stability of lithium thiophosphate solid electrolytes. Chemistry of Materials, 2019. 31(20): p. 8328-8337.

[10]. Sakuda, A., A. Hayashi, and M. Tatsumisago, Sulfide solid electrolyte with favorable mechanical property for all-solid-state lithium battery. Scientific Reports, 2013. 3(1): p. 1-5.

[11]. Grady, Z.A., C.J. Wilkinson, C.A. Randall, and J.C. Mauro, Emerging role of non-crystalline electrolytes in solid-state battery research. Frontiers in Energy Research, 2020. 8: p. 218.

[12]. Nagaev, K., Electron-electron scattering and conductance of long many-mode channels. Physica E: Low-dimensional

Systems and Nanostructures, 2018. 101: p. 144-150.

[13]. Mei, Q., B. Meyer, D. Martin, and S.W. Martin, Ion trapping model and the non-Arrhenius ionic conductivity in fast ion conducting glasses. Solid State Ionics, 2004. 168(1-2): p. 75-85.

[14]. Anantha, P. and K. Hariharan, Structure and ionic transport studies of sodium borophosphate glassy system. Materials Chemistry and Physics, 2005. 89(2-3): p. 428-437.

[15]. Kincs, J. and S.W. Martin, Non-Arrhenius conductivity in glass: Mobility and conductivity saturation effects. Physical review letters, 1996. 76(1): p. 70.

[16]. Bischoff, C., K. Schuller, S.P. Beckman, and S.W. Martin, Non-Arrhenius ionic conductivities in glasses due to a distribution of activation energies. Physical Review Letters, 2012. 109(7): p. 075901.

[17]. Deshpande, V., Factors affecting ionic conductivity in the lithium conducting glassy solid electrolytes. Ionics, 2004. 10(1): p. 20-26.

[18]. Kang, J., R. Gu, X. Guo, J. Li, H. Sun, L. Zhang, R. Jing, L. Jin, and X. Wei, Effect of SnO–P_2O_5–MgO glass addition on the ionic conductivity of Li1. 3Al0. 3Ti1. 7 (PO_4) 3 solid electrolyte. Ceramics International, 2022. 48(1): p. 157-163.

[19]. Gedam, R. and V. Deshpande, An anomalous enhancement in the electrical conductivity of Li_2O: B2O3: Al_2O_3 glasses. Solid State Ionics, 2006. 177(26-32): p. 2589-2592.

[20]. Anderson, O. and D. Stuart, Calculation of activation energy of ionic conductivity in silica glasses by classical methods. Journal of the American Ceramic Society, 1954. 37(12): p. 573-580.

[21]. McElfresh, D. and D.G. Howitt, Activation enthalpy for diffusion in glass. Journal of the American Ceramic Society, 1986. 69(10): p. C-237-C-238.

[22]. Zielniok, D., C. Cramer, and H. Eckert, Structure/property correlations in ion-conducting mixed-network former glasses: Solid-state NMR studies of the system Na_2O- B_2O_3- P_2O_5. Chemistry of materials, 2007. 19(13): p. 3162-3170.

[23]. Mohaghegh, E., A. Nemati, B.E. Yekta, and S. Banijamali, Effects of Fe_2O_3 content on ionic conductivity of Li_2O-TiO_2-P_2O_5 glasses and glass-ceramics. Materials Chemistry and Physics, 2017. 190: p. 8-16.

[24]. Zhang, J., C. Gao, C. He, L. Tan, S. Kang, Q. Jiao, T. Xu, and C. Lin, Effects of different glass formers on Li2S–P2S5–MS2 (M= Si, Ge, Sn) chalcogenide solid-state electrolytes. Journal of the American Ceramic Society, 2023. 106(1): p. 354-364.

[25]. Minami, T., Fast ion conducting glasses. Journal of Non-Crystalline Solids, 1985. 73(1-3): p. 273-284.

[26]. Fluegel, A., D.A. Earl, and A.K. Varshneya, Electrical resistivity of silicate glass melts calculation based on the SciGlass database. Independently Peer Reviewed, 2007. 1: p. 1-36.

[27]. Magistris, A., G. Chiodelli, and M. Duclot, Silver borophosphate glasses: Ion transport, thermal stability and electrochemical behaviour. Solid State Ionics, 1983. 9: p. 611-615.

[28]. Maass, P., M. Meyer, A. Bunde, and W. Dieterich, Microscopic explanation of the non-Arrhenius conductivity in glassy fast ionic conductors. Physical review letters, 1996. 77(8): p. 1528.

[29]. Zanotto, E.D. and J.C. Mauro, The glassy state of matter: Its definition and ultimate fate. Journal of Non-Crystalline Solids, 2017. 471: p. 490-495.

[30]. Guidotti, R.A., F.W. Reinhardt, and J. Odinek, Overview of high-temperature batteries for geothermal and oil/gas borehole power sources. Journal of power sources, 2004. 136(2): p. 257-262.

[31]. Wen, Z., Z. Gu, X. Xu, J. Cao, F. Zhang, and Z. Lin, Research activities in Shanghai Institute of Ceramics, Chinese Academy of Sciences on the solid electrolytes for sodium sulfur batteries. Journal of Power Sources, 2008. 184(2): p. 641-645.

[32]. Kumaravel, V., J. Bartlett, and S.C. Pillai, Solid Electrolytes for High-Temperature Stable Batteries and Supercapacitors. Advanced Energy Materials, 2021. 11(3): p. 2002869.

[33]. Schiefelbein, S.L., N.A. Fried, K.G. Rhoads, and D.R. Sadoway, A high-accuracy, calibration-free technique for measuring the electrical conductivity of

8

liquids. Review of scientific instruments, 1998. 69(9): p. 3308-3313.

[34]. Schiefelbein, S.L. and D.R. Sadoway, A high-accuracy, calibration-free technique for measuring the electrical conductivity of molten oxides. Metallurgical and Materials Transactions B, 1997. 28(6): p. 1141-1149.

[35]. Balcı, S., N.A. Sezgi, and E. Eren, Boron oxide production kinetics using boric acid as raw material. Industrial & engineering chemistry research, 2012. 51(34): p. 11091-11096.

[36]. Popescu, M.A., Medium range order in non-crystalline materials. J Ovonic Res, 2005. 1: p. 7-19.

[37]. Sopapan, P., R. Laopaiboon, J. Laopaiboon, P. Gunhakoon, T. Thongklom, and O. Jaiboon, Study of bagasse and cassava rhizome effects on the physical, mechanical and structural properties of soda-lime borate glasses. SN Applied Sciences, 2020. 2: p. 1-10.

[38]. Alajerami, Y., K. Abushab, S. Alagha, M.H.A. Mhareb, A. Saidu, F. Kodeh, and K. Ramadan, Physical and optical properties of sodium borate glasses doped with Dy 3+ ions. International Journal of Modern Physics B, 2017. 31(23): p. 1750171.

[39]. Bottelberghs, P. and G. Broers, Interfacial impedance behaviour of polished and paint platinum electrodes at Na2WO4-Na2MoO4 solid electrolytes. Journal of Electroanalytical Chemistry and Interfacial Electrochemistry, 1976. 67(2): p. 155-167.

[40]. Raistrick, I.D., C. Ho, Y.W. Hu, and R.A. Huggins, Ionic conductivity and electrode effects on β-PbF$_2$. Journal of Electroanalytical Chemistry and Interfacial Electrochemistry, 1977. 77(3): p. 319-337.